Hakimizad, A.; Raeissi, K.; Golozar, M.A.; Lu, X.; Blawert, C.; Zheludkevich, M.L.:

Influence of cathodic duty cycle on the properties of tungsten containing Al2O3/TiO2 PEO nano-composite coatings

In: Surface and Coatings Technology 340 (2018) 210 - 221
First published online by Elsevier: February 13, 2018

DOI: 10.1016/j.surfcoat.2018.02.042
https://dx.doi.org/10.1016/j.surfcoat.2018.02.042

Influence of cathodic duty cycle on the properties of tungsten containing Al_2O_3/TiO_2 PEO nano-composite coatings

Amin Hakimizad[a,*], Keyvan Raeissi[a], Mohammad Ali Golozar[a], Xiaopeng Lu[b, c], Carsten Blawert[b], Mikhail L. Zheludkevich[b, d]

[a] Department of Materials Engineering, Isfahan University of Technology, Isfahan 84156–83111, Iran

[b] Institute of Materials Research, Helmholtz-Zentrum Geesthacht, Max-Planck-Str. 1, Geesthacht, 21502, Germany

[c] Corrosion and Protection Division, Shenyang National Laboratory for Materials Science, Northeastern University, 3-11 Wenhua Road, Shenyang 110819, China

[d] Faculty of Engineering, University of Kiel, Kaiserstrasse 2, 24143 Kiel, Germany

(*Corresponding author, E-mail: a.hakimizad@ma.iut.ac.ir)

Abstract

Current waveforms with different cathodic duty cycles of 0, 20 and 40 % were applied to coat 7075 aluminum alloy in a silicate based electrolyte containing titania nano-particles. Using a constant current mode, the recorded voltage-time response showed that the required voltage for PEO coating process is lower in the presence of sodium tungstate as additive. By increasing the cathodic duty cycle, pancake surface morphology was converted to crater-like. Phase and chemical composition of the coatings were investigated by using grazing angle XRD and SEM/EDS. The tungsten concentration decreased linearly with the increase of cathodic duty cycle, which is dissimilar to the titania content. It was proposed that physical entrapping has been associated with electrophoretic incorporation of titania nano-particles, while the adsorption mechanism of tungstate anions is purely electrophoretic. Corrosion performance of the coatings was evaluated by potentiodynamic polarization and EIS

measurements. Addition of sodium tungstate was detrimental for corrosion performance of the coating in the case of unipolar waveform while the corrosion resistance was improved when bipolar waveforms were used. Long-term corrosion behavior of the coatings was investigated by EIS up to 16 weeks. The results showed remarkable difference between corrosion performance of the coatings produced by unipolar and bipolar waveforms, but the difference was negligible for the coatings produced by the bipolar waveforms with different cathodic duty ratios.

Keywords: Plasma electrolytic oxidation; 7075 Aluminum alloy; Pulse waveforms; Titania nano-particle; Sodium tungstate

1 Introduction

Plasma electrolytic oxidation (PEO) processing allows in-situ growth of oxide films by plasma discharges on the surface of valve metals in aqueous electrolytes [1-4]. Nowadays, this process is being optimized for fabricating thick, hard, and well-adhered oxide ceramic layers [5-9] with excellent wear resistance [3, 6, 10]. Such oxide coatings have wide variety of morphology and composition, excellent bonding strength to the substrate, good electrical and thermal properties [11]. The properties of PEO coating depends on various parameters, including electrolyte and electrical parameters.

One of the most important parameters is the applied waveform. It has been demonstrated that direct current (DC) mode produces thin and porous coatings [12]. A considerable improvement could not be seen by using pulsed unipolar waveform instead of DC for aluminum alloys [13, 14]. In fact, destructive discharges cause high porosity and low adhesion in PEO coatings produced by DC or unipolar waveforms. This kind of discharges

are found to be avoided by employing AC or bipolar power supplies [15]. Yerokhin et al. [9] reported that, compared to the AC process, the application of higher-frequency pulsed bipolar current results in increased coating growth rate. They found that the optimum range is 1 to 3 kHz region which provides better control over plasma discharges occurring at the sample surface and can reduce the volume fraction of the porous outer layer. Recently, much attention has been paid to 'soft' sparking of PEO, which is often observed at a selected AC or bipolar PEO conditions with higher cathodic current cycles with respect to the anodic current ones [15, 16].

The composition and concentration of the electrolyte are other important factors which determine the microstructure and properties of the coating. Various processes including chemical, electrochemical, thermodynamic and plasma-chemical reactions occur at the discharge sites due to increased local temperature (~ 10^3 to 10^4 K) and pressure (~ 102 MPa) [11], thus introducing ions into the discharges can change the coating composition, properties and microstructure. Many studies [5, 17-23] have confirmed that the electrolyte composition would directly affect the composition, structure, morphology and properties of the PEO coatings. Silicate based electrolyte is normally used to produce PEO coatings on Al alloy. Although SiO_3^{2-} has a strong adsorption capacity, allows to obtain greater growth rate and thicker ceramic coating, the stability of this electrolyte is poor and it usually results in rough coatings surfaces. Thus, in recent years many researchers have tried to improve the properties of PEO coating by adding additives to this electrolyte [17]. Additives are usually in the form of some metallic salts or nano/micro-particles. PEO coatings formed in the presence of ionic additives are favorable because of the unique effects of the additives on coating properties [16, 17, 22, 23]. For instance, the base electrolyte has been developed by adding potassium permanganate as a strong oxidizing agent [23], sodium tungstate as a neutral medium inhibitor [17] or ammonium metavanadate as a coloring agent [24]. It is also seen in literature

that the addition of $FeSO_4$ [16] into the base electrolyte for increasing the availability of oxygen and improving the combining chances of oxygen and aluminum, has positive effects on the resulted coating. The addition of particles into the electrolyte also influences the electrolyte characteristics, such as viscosity, which might have an effect on the coating morphology and properties. The particles can also contribute to the coating formation. They can incorporate inertly, partly reactive or reactively depending on their melting point [25, 26], size [25, 27] and the applied electrical parameters [28, 29].

In our previous work [14], the effect of titania nano-particles on surface morphology, composition and corrosion behavior of PEO coatings on 7075 Al alloy was studied using unipolar and bipolar waveforms with cathodic duty cycles of 20 and 40 %. By incorporation of TiO_2 nano-particles in the coatings, the coating thickness was slightly decreased, micro-cracks were developed and even became widen when unipolar waveform was applied. However, by using bipolar waveform at cathodic duty cycle of 40 %, the lowest porosity, and thus, the highest corrosion resistance was achieved at long-term immersion. PEO coatings with sodium tungstate (Na_2WO_4) additive are of interest because of their higher micro-hardness [17], catalytic, semiconducting and corrosion resistant properties [30]. The effect of adding both titania particles and sodium tungstate on photo-catalytic properties of the PEO coatings produced by DC current on Al from a similar silicate-based electrolyte are investigated by Tadić et al. [31]. However, the corrosion performance of the obtained coatings was not evaluated in this work. Moreover, the incorporation of the particles and contribution of ionic additives in the coating depend strongly on electrical parameters [29]. Thus, following our previous work [14] and similar to the ref. [31], we decided to study the effect of pulsed current regimes on microstructure and corrosion performance of the PEO coatings containing both titania particles and sodium tungstate. The influence of cathodic

duty cycle on uptake of tungstate ions and TiO_2 nano-particles and the resulting changes of coating microstructure and properties are also studied in this work.

2 Experimental procedure

2.1 Sample preparation

20 mm × 12 mm (Ø×H) cylindrical pieces of 7075 Al with chemical composition of 5.1 Zn, 2.2 Mg, 1.2 Cu, 0.3 Fe, 0.2 Si, 0.2 Cr and 0.2 wt. % Mn with remained aluminum were used as the substrate. The circumferences of the specimens were masked using epoxy adhesive and thermal shrink. Thus, only two flat sides of the cylindrical specimens were available for oxidation. The flat surfaces of all specimens were ground to average roughness of 0.08 µm using SiC abrasive papers. After degreasing in an acetone-charged ultrasonic cleaner and successively rinsing in deionized water, the samples were dried in warm air blow.

2.2 Plasma electrolytic oxidation

PEO process was carried out in 66 L of silicate based electrolyte consisting of 10 g L^{-1} Na_2SiO_3, 2 g L^{-1} KOH, 3 g L^{-1} TiO_2 nano-particles (rutile in spherical shape with average diameter of 30 nm) and 3 g L^{-1} sodium tungstate. The temperature of electrolyte was controlled indirectly in the range of 25±1 °C by aid of a R403 gas charged industrial double reciprocating compressor chiller. The pH of electrolyte was 12±0.1, measured using a digital pH-meter (AZ instrument model: 8651 PH & ORP Meter). Using a digital conductometer (SCHOTT CG 857), the conductivity of the electrolyte before and after addition of sodium tungstate additive were measured 5.51 and 7.06 mS respectively. Zeta potential of TiO_2 nano-particles was found about -45 mV using Zetasizer Nano ZS90 apparatus. The samples were coated using three different waveforms with cathodic duty cycles of 0, 20 and 40 %. All the

waveforms were applied for 1 h at 2 kHz with the average anodic (positive) current density of 5.6 A dm^{-2} for all waveforms and cathodic (negative) current density of 0, 5.6 and 11.2 A dm^{-2} for 0 %, 20% and 40% cathodic duty cycles respectively. During the PEO process, potential-time responses were recorded and a GPS 2042 digital oscilloscope was used to monitor the waveform shapes. The recorded waveforms, the bath composition, sample codes and coatings visual appearances are shown in Table 1.

2.3 Coating characterizations

The thicknesses of the coatings were measured using an eddy current coating thickness gauge (CEM DT-156); ten random measurements were taken from each coated surface followed by a statistical analysis to calculate the mean thickness value and standard variations. Surface roughness was evaluated using a profilometer (Mitutoyo SurfTest stylus working based on ISO 1997).

The phase composition of the samples was evaluated using a grazing angle X-Ray diffractometer (GAXRD, Bruker). The X-ray diffraction patterns were obtained over a 2θ range of 10–80 ° using Cu Kα radiation generated at 40 kV and 30 mA. The beam incident angles were 3, 5 and 10 °. X'pert Highscore software with PDF2 database was employed to analyze the patterns. A scanning electron microscope (SEM, TESCAN Vega3 SB) was used to study the surface morphology and cross-section of the specimens (which were sputtered with a thin gold layer in order to prevent surface charging effects [9]). The cross-sections were ground through successive grades of SiC papers and final polishing to 1 µm diamond. The coating surface was analyzed by energy dispersive spectroscopy (EDS, eumeX (IXRFsystems)) to determine the chemical composition. Elemental maps from the cross-section of the coatings were obtained using the same apparatus and an accelerated voltage of

15 kV was applied for SEM and EDS investigations. SEM (Philips XL30) was used to study the corroded surfaces of coatings.

2.4 Evaluation of corrosion behavior

The corrosion tests were performed using an AMETEK potentiostat/galvanostat (PARSTAT 2273). The tests were carried out in a three-electrode cell kit with a standard calomel electrode (SCE) as the reference electrode and a platinum plate as the counter electrode. The corrosion behavior of the coatings was evaluated by potentiodynamic polarization tests after 1 h immersion in 3.5 wt. % NaCl solution at pH 4, adjusted by adding HCl acid solution. The potential scan, which ranged from −250 to 1500 mV versus open circuit potential (OCP) at a scan rate of 1 mV s^{-1} was used for potentiodynamic polarization readings.

Electrochemical impedance spectroscopy (EIS) was used for further studying the corrosion behavior of the coatings, especially after long-term immersion up to 16 weeks in 3.5 wt. % NaCl solution (pH 4). The frequency-range of 10 kHz–100 mHz and 10 mV peak-to-peak voltage amplitude versus OCP were used for the measurements. The EIS data were analyzed using Zview software. In all tests, specimens with 2.54 cm^2 surface area were exposed to the corrosive solution, and each test was repeated at least three times.

Table 1: The visual appearance of the coated samples and the main effective parameters

Waveforms		**Bath (S3)**
Parameters	***Oscilloscope recorded graph***	***10 g L^{-1} Na_2SiO_3+2 g L^{-1} KOH + 3 g L^{-1} Nano-TiO_2 particles + 3 g L^{-1} Na_2WO_4***
Frequency=2 kHz Anodic duty ratio=20 %	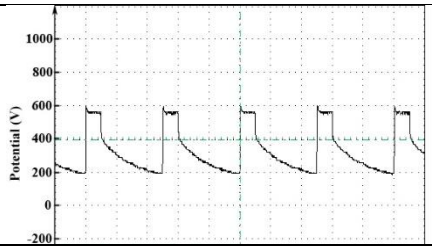	

Cathodic duty ratio=0 % (W1)		S3W1
Frequency=2 kHz Anodic duty ratio=20 % Cathodic duty ratio=20 % (W2)	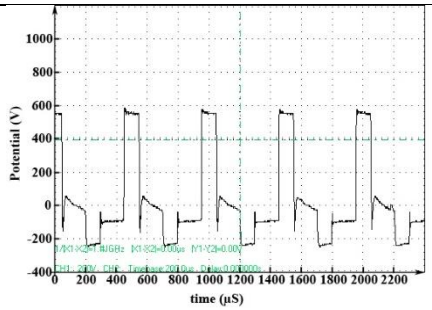	 S3W2
Frequency=2 kHz Anodic duty ratio=20 % Cathodic duty ratio=40 % (W3)	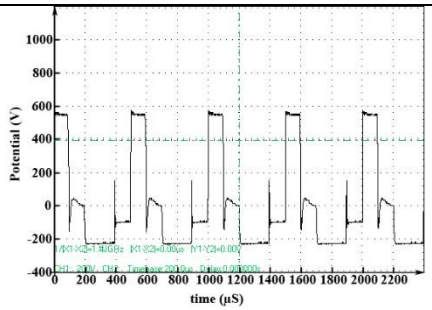	 S3W3

3 Results and discussion

3.1 Surface morphology observations

In Figure 1 a, related to the S3W1 specimen surface which is grown using unipolar waveform, cracks as long as 100 µm are obvious around and even in the center of the pancakes. The cracks become hair-like and shorter by applying 20 % cathodic duty cycle (S3W2 specimen, Figure 1b) and they are almost eliminated by using 40 % cathodic duty cycle (S3W3 specimen, Figure 1c). In our previous work [18], it was found that in the absence of sodium tungstate, the surface morphology of the titania-contained composite coating changed from a pancake to the crater-like by increasing cathodic duty cycle. In the presence of sodium tungstate, the bipolar waveforms can also decrease the number and size of micro-cracks, but, some craters and pancakes are still observed (Figure 1b and c).

Moreover, the bipolar waveform with cathodic duty cycle of 40 %, i.e. S3W3, has changed the surface morphology towards a higher numbers of craters (Figure 1c). The addition of sodium tungstate and increasing the cathodic duty cycle are both beneficial for reducing the micro-cracks and micro-pores but they may enhance the crater features. Similar to image analysis done in ref. [14], by assuming complete pancake morphology for the coating obtained by unipolar waveform (Figure 1a), the crater/pancake ratios are estimated by means of "Mipcloud image processing software" as 0.36 and 1.53 for S3W2 (Figure 1b) and S3W3 (Figure 1c), respectively.

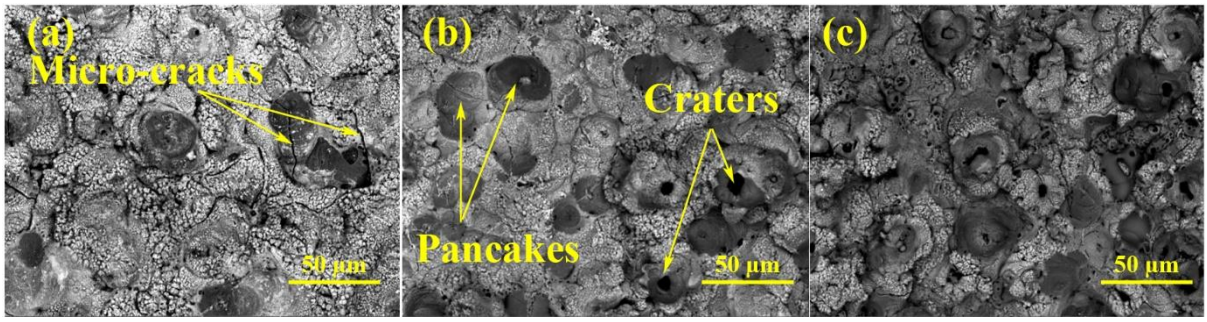

Figure 1: SEM surface morphologies of the coated specimens: a) S3W1, b) S3W2 and c) S3W3.

3.2 Coating thickness and roughness measurements

Figure 2 shows the thickness of the coatings produced by different waveforms. Approximately, a linear increase in thickness can be distinguished by increasing the cathodic duty cycle for the coatings obtained in tungsten-containing bath. PEO is a kind of anodizing process and it is expected that the growth phenomenon occurs only when the substrate is in anodic state. Therefore, the anodic part of the waveforms should be responsible for growing the oxide layer. However, the obtained results indicate that this may not be a true assumption. The thickness of S3W1 is ~ 33 µm using unipolar waveform with only anodic parts. In the case of bipolar waveforms, the sum of anodic parts is equal to that of unipolar, but they benefit from the different cathodic duties of 20 and 40 %, respectively. In this case, higher

thickness values (~ 37 and ~ 42 µm for S3W2 and S3W3 coatings, respectively) are obtained for these coatings as compared to S3W1. As seen, the bipolar waveforms provide higher coating thickness than the unipolar one.

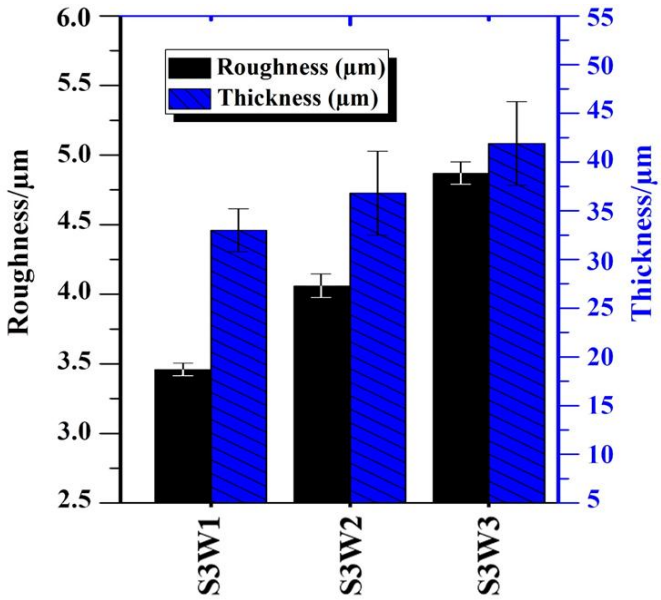

Figure 2: The coatings thicknesses measured using eddy-current technique and the relative surface roughness values (R_a).

Figure 2 also shows the roughness value of the coatings. The increase of the cathodic duty cycle increases the coating roughness. In agreement with literature [4, 11, 32], the surface roughness increases with increase of the coating thickness. For thicker layers of oxide coatings, higher energy is required for the current to pass through the coating. Under this condition, the current is localized at weak points of the formed layer to find its way. Consequently, the diameter of the discharge channels and molten oxide eruption increases resulting in a higher surface roughness [11].

3.3 Coatings cross-section observation

Figure 3 shows SEM cross-section images of the composite coatings produced in the presence of tungstate. Increasing roughness caused by increasing the cathodic duty cycle is

obvious from the cross-section images of the coatings, which are in a good agreement with Figure 2. However, due to the nature of eddy-current measurement which its accuracy may be affected by surface roughness and porosity, the thickness values obtained by SEM and eddy-current technique are not the same, but reasonably close to each other. S3W1 shows a network of the large pores in the substrate/coating interface which cannot be found in S3W2 and S3W3 coatings. These adjoined pores are called *"pore band"* [33], which is a sign of low coating/substrate adhesion [30]. A similar pore structure has been observed for the PEO coatings produced by DC current in a very similar electrolyte bath containing both titania particles and sodium tungstate [31]. In return, no "*pore band*" was detected in the absent of tungstate, according to our previous work [14]. This observation reveals that the sodium tungstate changes not only the surface morphology, but also the porosity features of the coatings. Figure 3b shows cross-section of S3W2, which reveals some discrete micro-pores instead of the pore band. This demonstrates that the bipolar waveform can also modify the pores structure. In Figure 3c, the porosity is obviously low. It is clear that the increase of cathodic duty cycle has a significant effect on decreasing level and structure of the pores, which also enhancing the adhesion of the composite coatings. Overall, it can be concluded that in the presence of sodium tungstate, using the bipolar pulsed waveform with a wide cathodic duty cycle is essential for producing high quality PEO coatings.

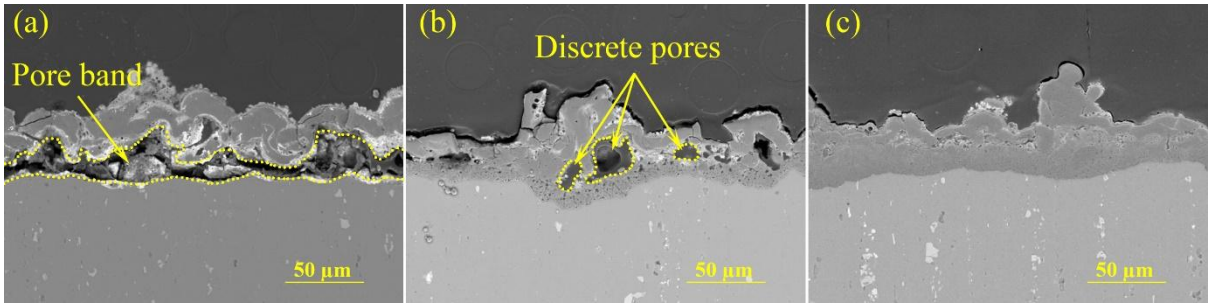

Figure 3: SEM cross-section images of the tungsten-containing composite coatings a) S3W1, b) S3W2 and c) S3W3

3.4 Compositional and phase analyses of the coatings

Figure 4 shows GAXRD patterns of the coatings at different waveforms. As seen, the coatings show γ-alumina and rutile plus metallic tungsten for all waveforms. During the PEO process, rapid solidification of molten alumina favors the formations of γ-Al_2O_3 [4, 11]. The mullite (alumina-silicate) has chance to be formed in crystalline structure because the molten alumina can react with silicate ions present in the electrolyte bath [34]. The most stable phase among mullite, γ and α alumina phases is α-alumina which needs higher temperature to form. The molten alumina may also produce α-alumina instead of γ-alumina (directly or through γ→α phase transformation), where the presence of titania nano-particles facilitates the phase transformation [12]. However, the formation of mullite or α-alumina needs enough energy which should be provided by the plasma discharges during the PEO process [23]. In Figure 4, there are no peaks related to α-alumina in the patterns, thus it can be concluded that the applied energy was not high enough to transform γ-alumina to α, and even, the catalytic role of titana nano-particles was not effective for encouraging this transformation. The obtained result is in agreement with ref. [2], where the lower duty cycle of pulsed waveform resulted in lower ratio of α-alumina/γ-alumina. It should be mentioned that the dependency of the phase composition to the current mode is not limited to Al alloys and it has also been reported for Ti [35] and Mg alloys [36, 37]. In the present study, 7075 aluminum alloy was used as the substrate which has a considerable amount of alloying elements, thus, the effects of these elements especially Zinc should also be taken into account and not only the lower applied energy for preventing α-alumina formation as mentioned in refs. [12, 14].

Although there are some reactions that have been suggested for the formation of WO_3 [4], eventually, WO_3 can react with Al under high temperature condition by the following

chemical reaction [4, 38-41] proceeding due to the fact that the Al is abundant in the discharge channels:

$$WO_3 + 2Al \rightarrow Al_2O_3 + W \quad (1)$$

In the present study, the formation of pure W in the coatings was confirmed by XRD patterns (Figure 4) too. However, very low concentration of tungstate in the electrolyte and high dispersion of tungsten containing species over the surface prevent the detection of tungsten species in the coating [31]. It seems that the presence of tungsten in the composition or contribution of tungstate ions in plasma discharges has facilitated the reaction of the molten alumina with silicate ions and formation of mullite which is completely in accordance with ref [42]. By applying the bipolar waveforms, the intensity of the peaks related to tungsten drops significantly with subsequent disappearing of the mullite. This emphasizes the catalytic effect of tungstate on formation of mullite. By increasing the cathodic duty cycle from 20 to 40 %, the coating composition remains almost constant, but nearly, the peaks related to tungsten are eliminated from the patterns. This is related to the wider cathodic cycle. The anions such as tungstate are more repulsed using wider cathodic cycle and contribute less in the coating formation.

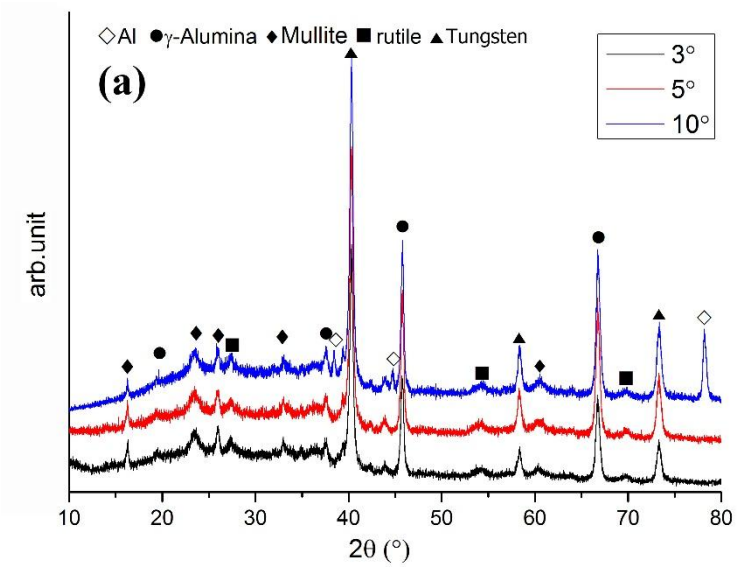
◇Al ●γ-Alumina ♦Mullite ■ rutile ▲Tungsten
(a)
3°
5°
10°
arb.unit
10
20
30
40
50
60
70
80
2θ (°)

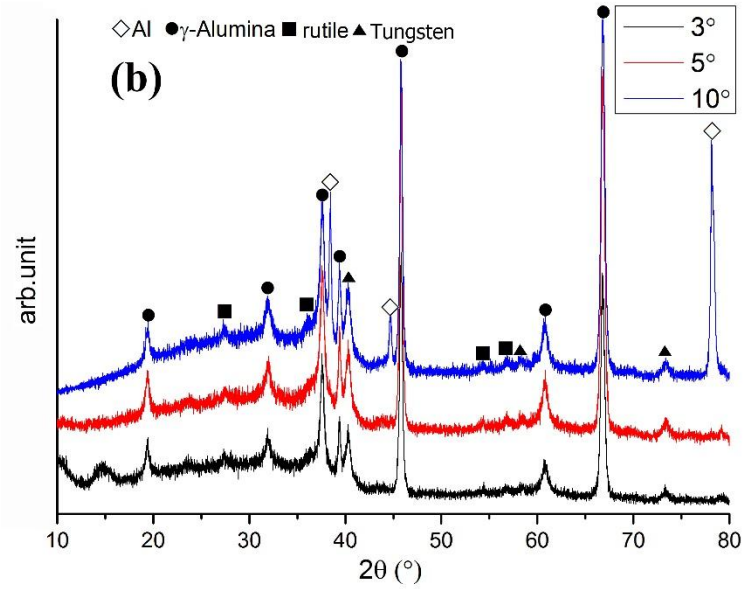
◇Al ●γ-Alumina ■ rutile ▲Tungsten
(b)
3°
5°
10°
arb.unit
10
20
30
40
50
60
70
80
2θ (°)

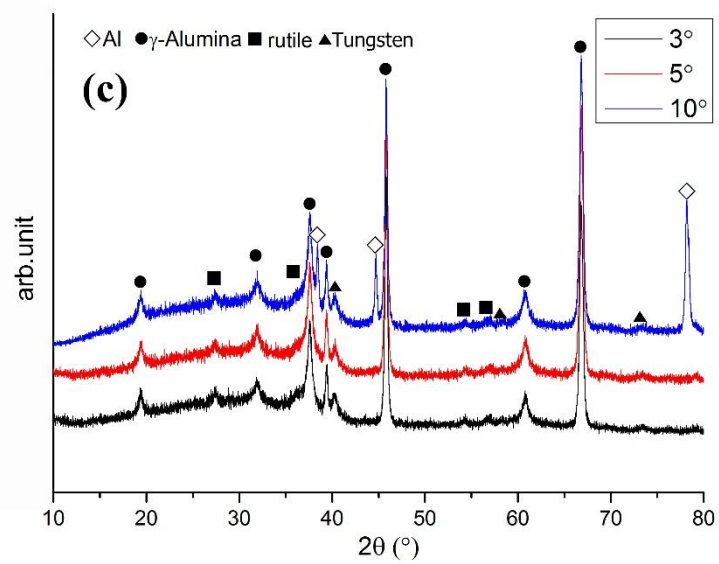

Figure 4: The GAXRD patterns of W containing composite coatings, a) S3W1, b) S3W2 and c) S3W3.

3.5 EDS analysis and elemental maps

Figures 5-7 show the elemental maps on cross sections of S3W1, S3W2 and S3W3 coatings. More uniform distribution of Ti rather than W element is confirmed from the maps. However, some localized areas with higher Ti concentration can be distinguished, especially in the boundaries of the pores. This may be due to sample preparation which creates accumulation of detached nano-particles on cross-sections during polishing or by particles entering into the open pores during PEO processing. The latter is much more likely.

It is obvious that the tungsten is not distributed uniformly in the cross-section of the coatings and some enriched areas are evident as well as some depleted zones. The interesting finding is the similarity between distribution maps of tungsten and silicon elements. By reconsidering the figures, it can be concluded that by using the bipolar waveforms, these elements are distributed more uniform in the coatings (S3W2 and S3W3). The reason is the frequent adsorption and repulsion of these ions during anodic and cathodic cycles, respectively. This

strongly confirms that the incorporation of electrolyte elements (tungsten and silicon) in the coating is based on the electric force.

By considering EDS data in Table 2, it is seen that the incorporation of titania nano-particles in the coatings does not show a reasonable correlation with increasing cathodic duty cycle. The results is in agreement with the composite coatings obtained previously in additive-free bath [14]. However, regarding the tungsten, its concentration decreases linearly by increasing the cathodic duty cycle, in accordance with visual observation of the coatings brightness, elemental maps and also GAXRD results. As seen in Table 1, the coating produced by unipolar waveform (S3W1) is darker than S3W2 and S3W3 coatings produced by the bipolar ones at the same condition. If the tungsten content decreases, the coatings will be brighter as mentioned in ref. [42]. It has been reported that the color intensity depends on the tungstate concentration in the electrolyte, but it also highly depends on the current pulse mode [42]. Since TiO_2 nano-particles are distributed more uniformly in the coatings and because its concentration has not changed reasonably with the waveforms, it can be concluded that the embedding of TiO_2 nano-particles into the coatings is not just through electrophoretic force. This also happened when DC waveform was used in our previous study [12]. For the particles to participate in the PEO coating, they need to be transferred into the electrolyte/coating interface with the aid of an external force. The contribution of particles in the PEO coating can be divided into two steps including uptake and incorporation. For the uptake step, one of the most promising factors which bring the particles near the anode is electrophoretic force [26, 27]. The electrophoretic mobility and mechanical stirring are mentioned as the main factors for particle movements [43]. The electrophoretic force depends on zeta potential value and its magnitude dictates the degree of electrostatic repulsion between the adjacent particles inside the solution. The particles with higher absolute values of zeta potential are more stable, and this prevents them from agglomeration and settling in electrolyte solution. It is found that

most of the particles are fortunately negatively charged (show negative zeta potential) after dispersion in the alkaline electrolyte and surrounding by hydroxyl ions [26, 27]. Thus, it is expected that the amount of incorporated particles is in direct relation with the applied voltage or current density, since the dispersed particles are negatively charged and they should move towards the anode continuously [29]. In the present study, if the electrophoretic mobility be assumed as the only way for incorporation of nano-particles into the coatings, thus, lower incorporation of nano-particles should be seen when the bipolar waveforms are applied. Thus, it can be concluded that comparing mechanical stirring and electrophoretic force for incorporating the particles, the former overcomes the latter in our study. The reason is the high stirring intensity of the centrifugal pump applied here in comparison with magnetic stirrers or bubbling generators used commonly in laboratory PEO process [25, 27]. When the stirring is not strong enough, the dispersing and uptaking of particles in the electrolyte are controlled by electrophoretic force as described in many references [25-29, 33]. In current study, it seems that although the zeta potential of titania nano-particles is low enough (~ -45 mV), the strong stirring provided by centrifugal pump diminishes the role of electrophoretic force. However, our results showed that this vigorous stirring cannot eliminate the electric force which supports the ions migration. In contrast to the nano-particles, the amount of tungsten and silicon is reduced linearly with increasing cathodic duty cycle of the bipolar waveform in agreement with EDS and GAXRD results. In fact, with the wider cathodic cycle, the contribution of electrolyte anions in the oxide formation during PEO process decreases and thus their constituent elements (W and Si) in the coatings will be lower (Table 2). It is known that the PEO coatings grow using both substrate and electrolyte constituents, thus, reducing the contribution of electrolyte constituents means increasing contribution of substrate constituents. However, unlike the unipolar waveform which encourages the anions attraction, the bipolar waveforms tend to consume both anions and

cations. Therefore, Al^{3+} ions may incorporate more in the coating using the bipolar waveforms. These are the reasons for the higher Al concentration found in the bipolar grown coatings as seen in Table 2.

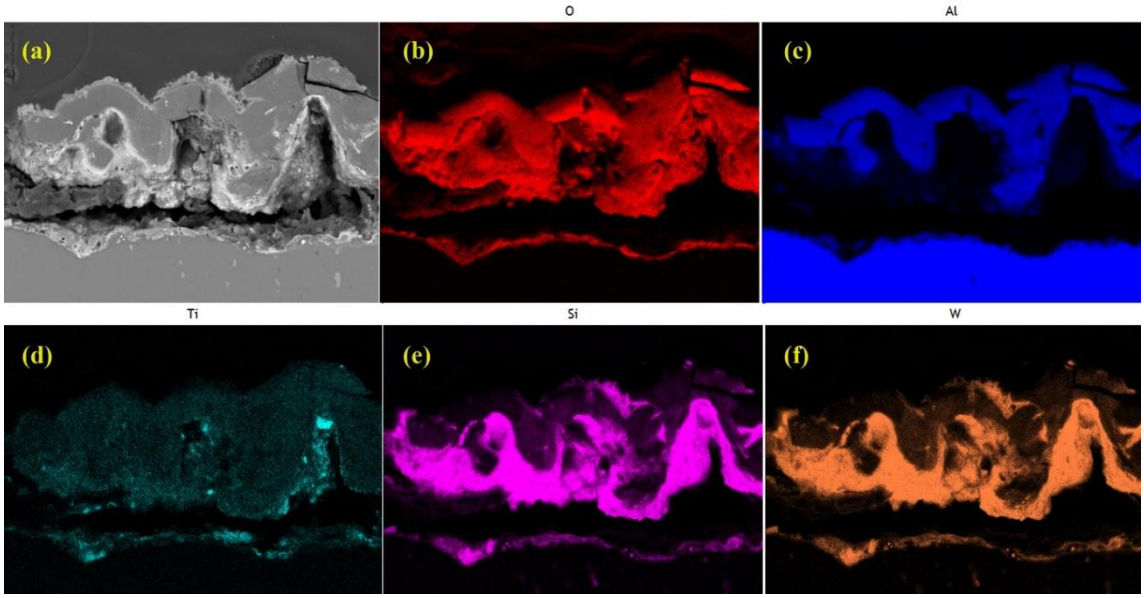

Figure 5: Cross-section elemental mappings of S3W1 specimen a) SEM image of mapped area, b) map of oxygen, c) map of aluminum, d) map of titanium, e) map of silicon and f) map of tungsten

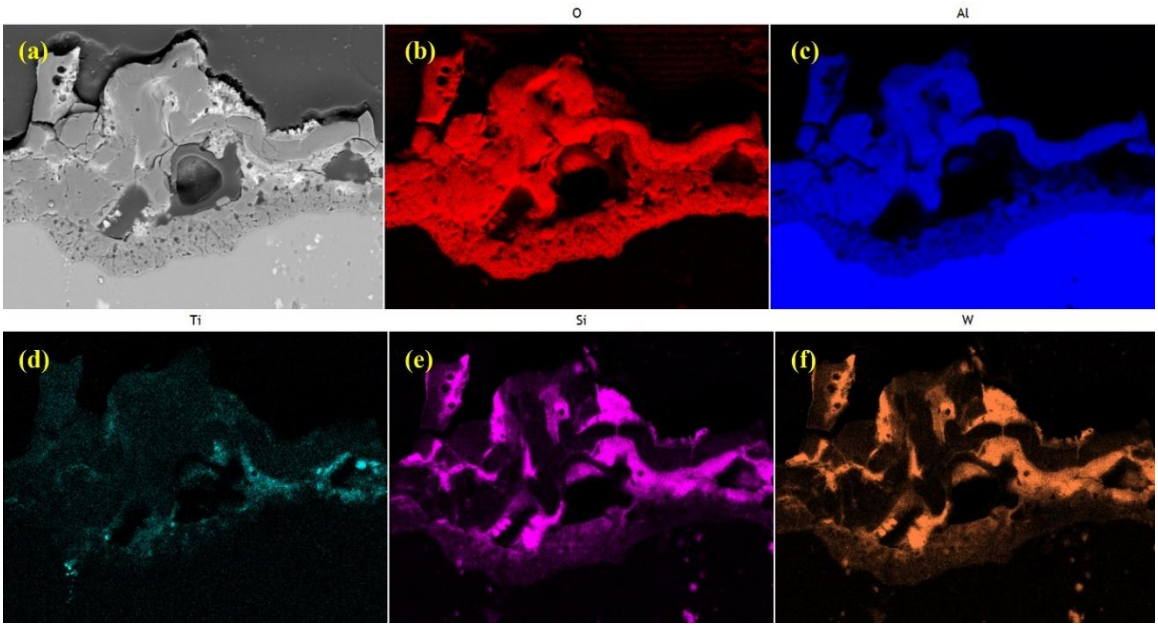

Figure 6: Cross-section elemental mappings of S3W2 specimen a) SEM image of mapped area, b) map of oxygen, c) map of aluminum, d) map of titanium, e) map of silicon and f) map of tungsten

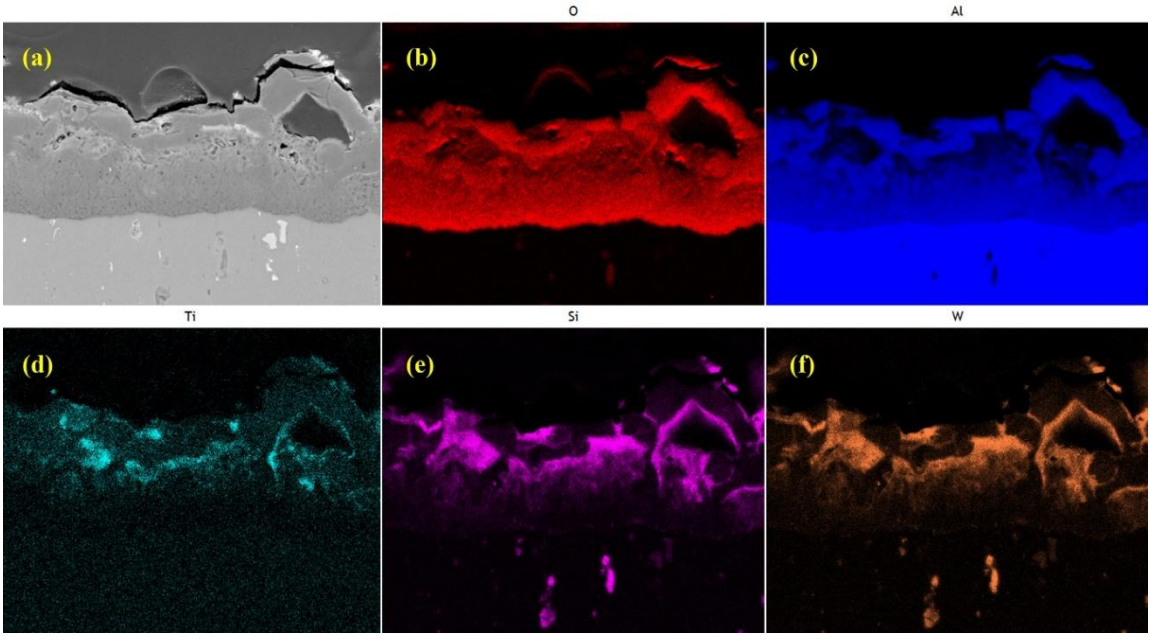

Figure 7: Cross-section elemental mappings of S3W3 specimen a) SEM image of mapped area, b) map of oxygen, c) map of aluminum, d) map of titanium, e) map of silicon and f) map of tungsten

Table 2: Surface composition (at. %) of PEO coatings determined by EDS analysis

Coating	O	Na	Al	Si	K	Ti	W
S3W1	57	1.5	11	23	1.5	2.8	2.4
S3W2	54	2.1	21	18	1.4	1.5	1
S3W3	55	2.5	20	17	2	2.5	0.5

3.6 Corrosion behavior of the coatings

3.6.1 Potentiodynamic polarization tests

Potentiodynamic polarization technique was employed to investigate the corrosion performance of the coatings in 3.5 wt.% NaCl solution (adjusted at pH 4 using hydrochloric acid). The potentiodynamic polarization curves of the coatings after 1 h immersion are shown in Figure 8. In the polarization curves, the cathodic response is due to the oxygen reduction reaction while the anodic one is related to the repassivation reactions occurred in the oxide coating and/or anodic dissolution of aluminum limited by IR drop through the PEO layer which is in turn proportional to the barrier properties of the films and dependent on their stability. A rapid increase of anodic current is seen for the uncoated alloy, suggesting that the sample cannot be passivated because of the onset of localized corrosion. A very high anodic current is also measured for the sample coated by unipolar waveform at higher potentials suggesting that the coating does not protect the substrate properly and does not ensure sufficient barrier properties as also later demonstrated by EIS results. In contrast, when PEO was performed using the bipolar modes, lower current values can be observed demonstrating good barrier properties of the layers and their high stability. Notably, the polarization curve

for the S3W3 coating is laid at the lowest current densities indicating its best corrosion performance. However, both coatings grown by the bipolar waveforms show passive behaviors. For S3W3 coating, no sign of localized attack even at very high potentials can be detected. This behavior is so different from the polarization behavior observed for S3W1.

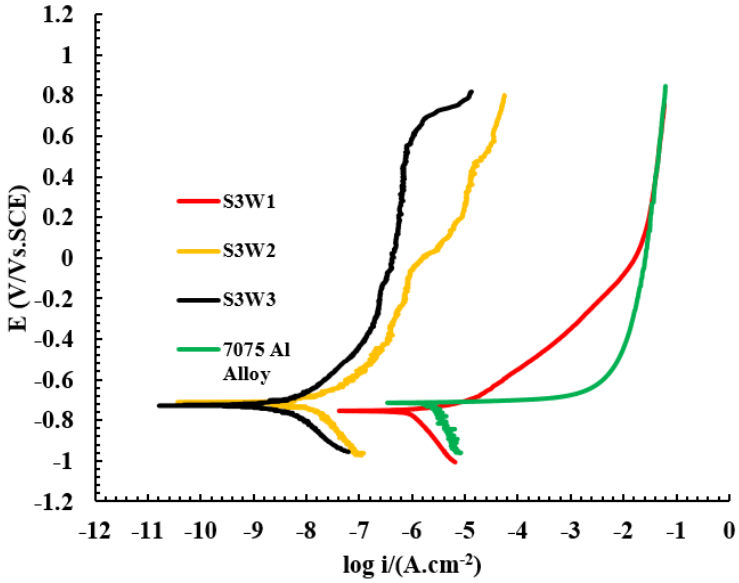

Figure 8: Potentiodynamic polarization curves for the coated specimens and 7075 aluminum alloy substrate. The tests are performed in 3.5 wt % NaCl solution at pH 4 after 1 h immersion at scan rate of 1 mV s^{-1}.

According to Figure 8, the PEO coating produced in the presence of tungstate using unipolar waveform is not beneficial for corrosion protection of 7075 Al alloy. In this case, the corrosive solution could easily penetrate into the coating and reach the substrate surface, i.e. there is no efficient barrier against the penetration of corrosive solution. The results are in accordance with the cross-sectional observations, where the higher density of pores and also the "*pore band*" were obviously seen in cross-section of S3W1 coating (Figure 4). In contrast, for the coatings produced using the bipolar waveforms, the corrosion performances are considerably higher than that provided by the unipolar one. It is seen that the presence of

cathodic part of the waveform plays a significant role on improving the corrosion performance of the coating by preventing the pore band formation, where the wider cathodic cycle also creates the less porous oxide layers providing more effective barrier.

There are two suggested mechanisms on the positive effects of cathodic part of a bipolar waveform named “randomizing the breakdowns” and “sealing effect”. The former is due to the unique effect of cathodic cycles of the bipolar waveforms which randomizes the sites of succeeding anodic breakdowns. The repetition of breakdowns in the same locations leads to the localized breakdown areas which promotes the formation of large discharge channels [15]. Additionally, it can promote the formation of “*pore band*” and lead to coating spallation during the PEO process. Therefore, the coatings produced using DC [12] and unipolar waveforms, which provide no cathodic parts, are more porous. The present study along with our previous work [14] show that the bipolar waveforms lead to higher compactness and thickness of the PEO composite coatings on 7075 Al alloy. The latter mechanism is sealing where cathodic pulse which follows an anodic one can seal the cracks and discharge channels left by the anodic pulses [42]. Hydrogen liberation and alkalization of adjacent electrolyte regions are old assumptions which can be supposed for the sealing mechanism [44, 45], but the details of mechanism needs more study. Both of these mechanisms should increase the coatings corrosion performance. The results show that the sodium tungstate enhances the necessity of applying the cathodic duty cycles. The results are in accordance with the results of Mann et al. [42], in which the highest corrosion performance of the coatings was achieved by simultaneous application of tungstate and high frequency bipolar pulses, where the coating produced by unipolar pulse showed poor corrosion performance. Xiang et al. [30] have also reported higher corrosion performance of the coatings in the presence of sodium tungstate by using the bipolar waveform. Regarding the results obtained in current research and those found in the literature [30, 42], it is concluded that the effect of sodium tungstate on the

corrosion performance of the coatings depends on the mode of the applied waveform. In this study, sodium tungstate may act deterioratively or constructively by using unipolar and bipolar waveforms, respectively. Similarly, titania nano-particles are also found beneficial for improving the corrosion performance of the obtained coatings if the bipolar waveforms are applied, but, they are deteriorative if the unipolar waveform is applied [14].

3.6.2 Electrochemical Impedance Spectroscopy measurements

Electrochemical impedance spectroscopy (EIS) was used for better understanding and comparing the corrosion performance of the coatings produced at different conditions at long immersion times from 1 h up to 16 weeks. It should be noticed that the corrosion behavior at OCP is different from that of the polarized conditions. In polarization readings, due to the positive electrical field applied at anodic condition; diffusion of Cl^- ions from bulk solution into the pores is possible. This means that a higher concentration of aggressive solution will attack the substrate. However, in EIS tests at OCP condition, the substrate is attacked by the penetrated solution with almost similar ion concentrations as the bulk electrolyte. Figure 9 shows EIS diagrams after different immersion times. Figure 10 illustrates the equivalent electrical circuits used for fitting the EIS data.

PEO coatings is usually composed of an outer porous layer and an inner barrier layer. Accordingly, there are two time constants for PEO coatings in EIS tests corresponding to response of these two layers [11, 21]. In our study, because of the presence of “pore band” in the unipolar coated specimen, the outer porous layer misses its effective role in corrosion performance, while for the bipolar coated specimens, both outer and inner layers show high resistances indicating good barrier properties. However, the corrosion of Al substrate is just possible for the coating grown by the unipolar waveform. Accordingly, two different equivalent circuits are used for fitting data as seen in Figure 10a and b. These two equivalent

circuits are well known and commonly used for PEO coatings [21, 30, 46-49]. Actually, the connected pores as "*pore band*" found in S3W1 create easy pathways for corrosive solution to reach the substrate and are responsible for appearing a constant phase element related to electrical double layer (CPEdl) parallel with charge transfer resistant (Rct), respectively. Table 3 shows the fitted data from EIS tests after 1 h immersion using the models represented in Figure 10. In accordance with the polarization test results, the inner layer resistance (R_{in}) of the coatings produced using the bipolar waveforms are significantly higher than the coatings produced by the unipolar waveform. For S3W3 specimen, there is no doubt that its higher compactness plays the major role for achieving the highest R_{in} and outer layer resistance (R_{out}) values (Table 3), and thus, the highest corrosion performance.

GAXRD and EDS results show that increasing the cathodic duty cycle decreases the incorporation of tungstate ions in the process, and thus, tungsten in the coatings composition. Xiang et al. [30] have reported that the presence of sodium tungstate as an additive improves the corrosion resistance of PEO coatings against corrosive environment, which may be attributed to the abundant oxygen available for the oxide formation leading to smooth surface with fewer defects. If sodium tungstate is assumed beneficial, the increase of its contribution should raise the corrosion performance of the coatings. By considering Table 3, this behavior is not seen. It shows that although W1 waveform has led to maximum incorporation of tungstate ions, the corrosion performance of S3W1 is much lower than S3W2 and S3W3, thus, it can be concluded that the coating morphology and its pores structure determine the corrosion performance of the PEO coatings, not the amount of incorporated tungsten. This result is in agreement with ref. [11], which has reported that neither the tungsten content nor the thickness of the coatings are identified as the important factors in determining the corrosion performance of PEO coatings. In fact, the morphology and pores structure play the major roles.

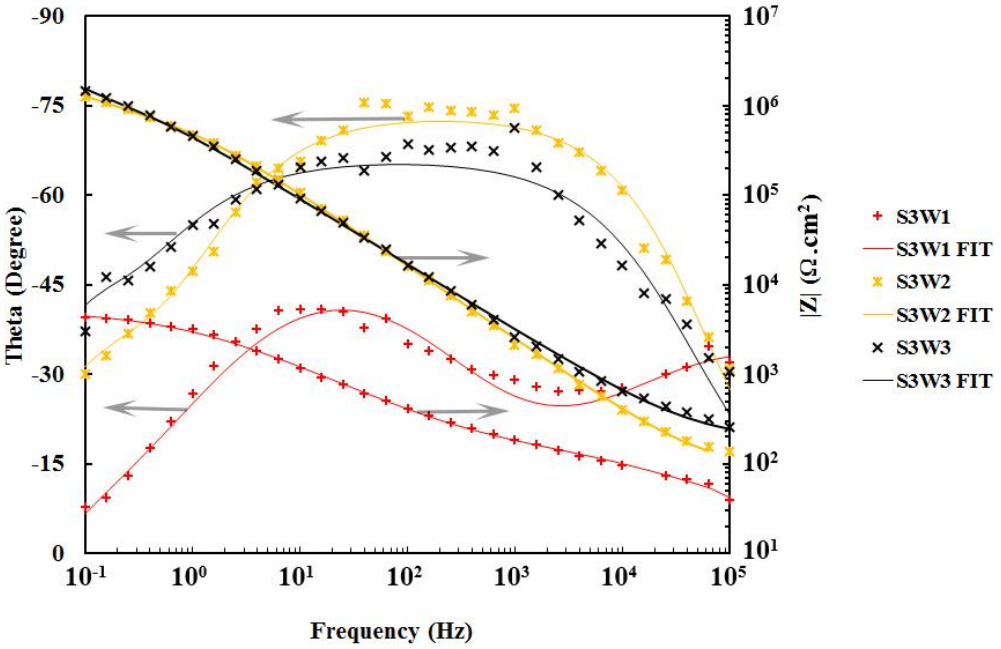

Figure 9: Bode plots of PEO coatings after 1 h immersion in 3.5 % NaCl with at pH 4.

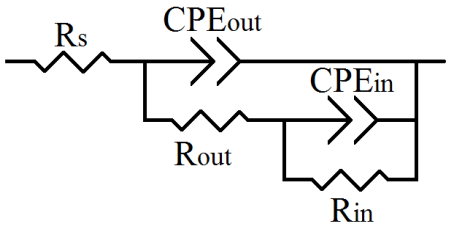

a

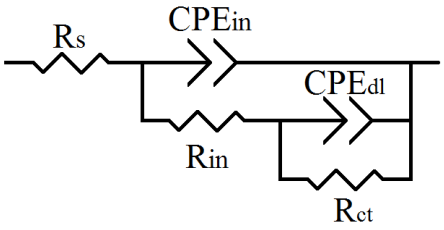

b

Figure 10: Equivalent electrical circuit used to fit the EIS data of PEO coated specimens, Rs: uncompensated solution resistance, Rout: outer porous layer resistance, CPEout: constant phase element of outer porous layer, Rin: inner compact layer resistance, CPEin: constant phase element of inner compact layer, Rct: the resistance of charge transfer and CPE_{dl}: constant phase element for electrical double layer.

Table 3: Fitting results of EIS data for the PEO coatings after 1 h immersion in 3.5 % NaCl at pH 4

Specimen Code	Porous outer layer			Inner compact layer			Charge transfer		
	CPE_{out}		R_{out}	CPE_{in}		R_{in}	CPE_{dl}		R_{ct}
	T ($\mu F.cm^{-2}.S^{n-1}$)	P	($k\Omega.cm^2$)	**T ($\mu F.cm^{-2}.S^{n-1}$)**	P	($k\Omega.cm^2$)	**T ($\mu F.cm^{-2}.S^{n-1}$)**	P	($k\Omega.cm^2$)
S3W1	-	-	-	18.36±1.3	0.531± 0.037	0.187±0.013	45.5±3.18	0.622 ± 0.042	4.975±0.348
S3W2	0.32±0.013	0.816± 0.033	903.610± 36.15	1.294±0.05	0.763± 0.031	1462±60	-		-
S3W3	0.520±0.016	0.734± 0.02	2044.5± 61.33	1.100±0.033	0.96± 0.03	1643±50	-		-

Figure 11 shows the variation of the R_{in} of the S3W1, S3W2 and S3W3 versus immersion time in 3.5 wt % NaCl solution. The R_{in} of S3W1 is very low and it remains low during long-term immersion with just a negligible increase which is due to accumulation of corrosion product in the pore band and passible formation of an artificial barrier. However, the R_{in} values of S3W2 and S3W3 are increased gradually after the first sudden drop during the test. The reason is believed to be the repairing mechanism [48], which is also called "self-healing" [26]. The inert incorporated TiO_2 particles has been beneficial for donating self-healing functionality to the PEO coatings by prompting the hydroxide phases [26]. This reported for the composite coatings with no tungsten content before [14]. In some cases, the added particles are not effective or even they are deteriorative for the corrosion performance of the coatings during long-term corrosion tests because of the higher porosity created by them, especially at higher contents [26]. However, the process of repairing mechanism is more possible for the coatings with relatively small defects which can easily be blocked [50]. After 16 weeks of immersion, S3W2 and S3W3 specimens retain their high resistances (Figure 12).

This means that the composite coatings containing tungsten had the ability to protect the substrate by slowing down the penetration of aggressive Cl^- even up to 16 weeks of immersion.

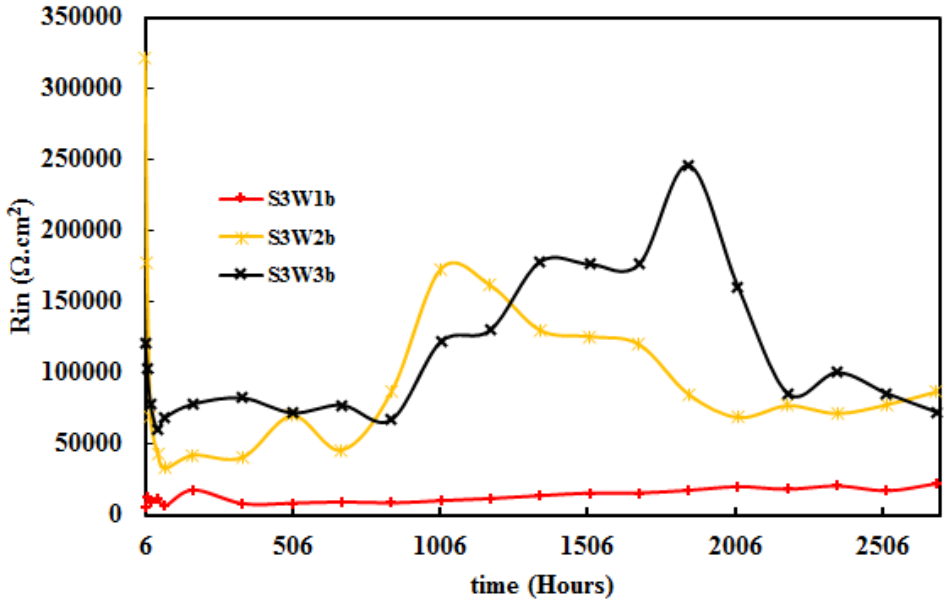

Figure 11: The variation of R_{in} versus time for the coatings during immersion in 3.5 % NaCl solution at pH 4.

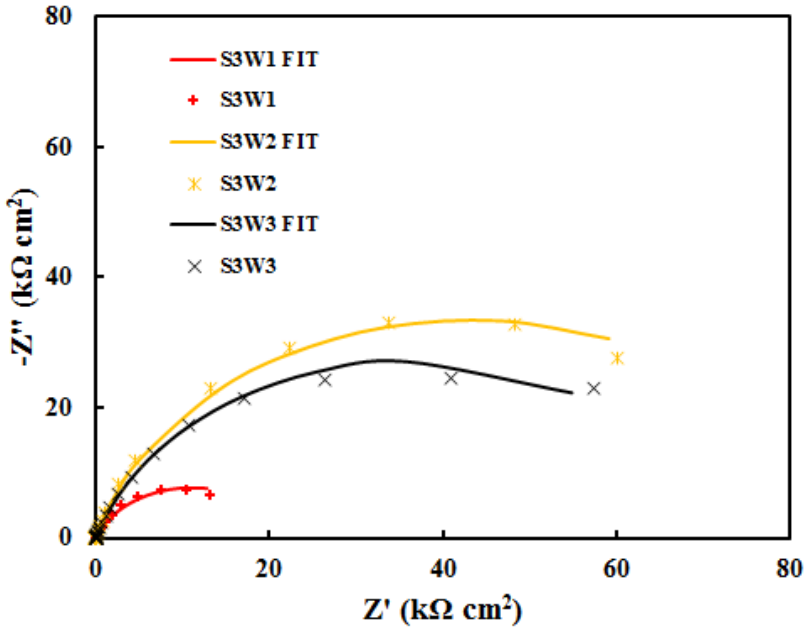

Figure 12: Nyquist plots of the PEO coatings after 16 weeks immersion in 3.5 % NaCl adjusted at pH 4.

SEM images from surface and cross-section of the specimens immersed up to 16 weeks are presented in Figure 13. As seen, for the coatings produced by the bipolar waveforms (S3W2 and S3W3), no obvious dissolution can be detected inside the coating or at the coating/substrate interface. However, it seems that a slight dissolution has occurred through the pore band in S3W1. This means that the corrosion reactions have proceeded beneath the coating, although the coating surface did not undergo significant changes.

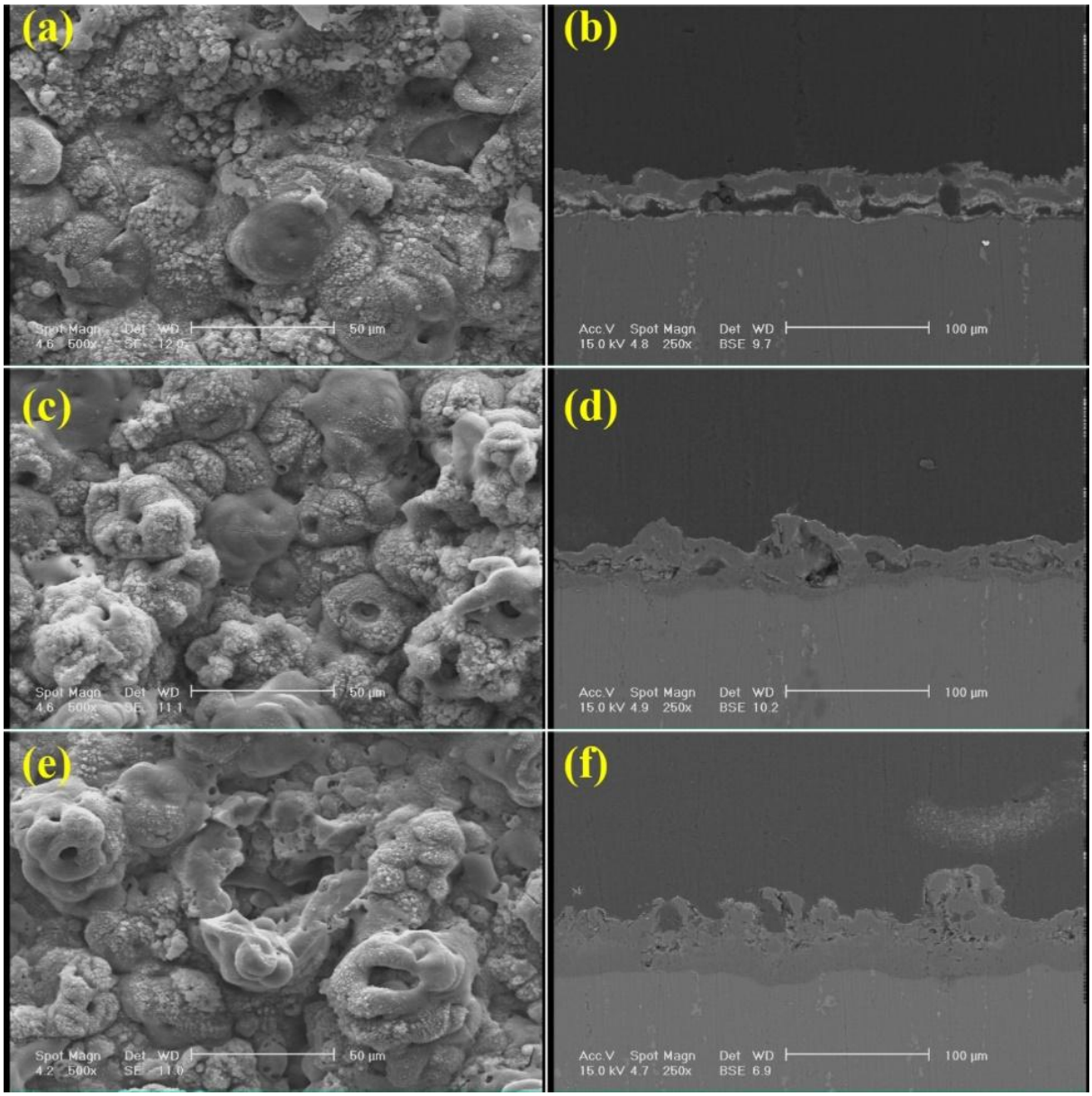

Figure 13: SEM images of the surface and cross-section of the coated specimens after 16 weeks immersion in 3.5 wt.% NaCl adjusted at pH 4. a, b) S3W1, c, d) S3W2 and e, f) S3W3.

4 Conclusions

Sodium tungstate was added to the electrolyte containing TiO_2 nano-particles (30 nm) as an additive and three different waveforms were used to produce PEO coatings on 7075 Al substrate in the resultant electrolyte. Following results can be obtained from evaluation of the process and the coatings.

1- Adding sodium tungstate into the electrolyte decreased voltage during all steps of the PEO process using all waveforms.
2- The unipolar waveform produced pancake-like morphology, while using bipolar mode lead to crater-like morphology.
3- Contribution of tungstate ions in PEO process and using a higher cathodic duty cycle led to a less porous morphology without the presence of pore band in the coatings.
4- The compactness, roughness, thickness and thus growth rate of the coatings increased by increasing the cathodic duty cycle.
5- Electric adsorption is the dominant mechanism for incorporation of tungstate ions and physical entrapping associated with electrophoretic incorporation of titania nano-particles. The vigorous mechanical mixing which encourages the physical trapping, did not disturb the electric forces, and thus, did not interfere with the ions incorporation. Hence, the anions response well to the waveform polarity changes. However, this overcame the electrophoretic forces for the nano-particles.
6- The cathodic duty cycle of the waveform not only changed the morphology and pores structure of the coatings, but also it changed the chemical composition of the coatings.
7- Applying the bipolar waveform eliminated the “pore band” at substrate/coating interface. Accordingly, the bipolar coated samples showed better corrosion performance than that obtained by the unipolar waveform. Both coatings grown by

the bipolar waveforms showed passive behaviors. For the coating grown by wider cathodic duty cycle, stronger passivation was observed with no sign of localized attack even at very high polarized potentials during the polarization test.

8- The inner layer resistances of the coatings produced using the bipolar waveforms are significantly higher than the coating produced by the unipolar waveform. The outer porous layer in the unipolar coated specimen missed its effective role in corrosion performance because of the presence of "pore band", while this layer acted as an effective barrier for the bipolar coated specimens. This highlights the role of the pore structure on corrosion performance of the PEO coatings.

Acknowledgment

Supports from Iran Nanotechnology Initiative Council (84768) and Isatis Nano Plating Co. are gratefully acknowledged. In addition, authors are thankful from Yekta Mobaddel Pars Co. for programing the waveforms. X. Lu would like to acknowledge the financial support of the Young Elite Scientists Sponsorship Program by CAST (2017QNRC001) and National Natural Science Foundation of China (NO. U1737102).

References

[1] V. Shoaei-Rad, M.R. Bayati, H.R. Zargar, J. Javadpour, F. Golestani-Fard, Materials Research Bulletin, 47 (2012) 1494-1499.
[2] V. Dehnavi, X.Y. Liu, B.L. Luan, D.W. Shoesmith, S. Rohani, Surface and Coatings Technology, 251 (2014) 106-114.
[3] Y.-l. Cheng, M.-k. Mao, J.-h. Cao, Z.-m. Peng, Electrochimica Acta, 138 (2014) 417-429.
[4] S. Stojadinovic, R. Vasilic, I. Belca, M. Petkovic, B. Kasalica, Z. Nedic, L. Zekovic, Corrosion Science, 52 (2010) 3258-3265.
[5] X. ShiGang, L. Jun, S. LiXin, Key Engineering Materials, 512-515 (2012) 1082-1088.
[6] V. Shoaei-Rad, M.R. Bayati, F. Golestani-Fard, H.R. Zargar, J. Javadpour, Materials Letters, 65 (2011) 1835-1838.
[7] S. Sarbishei, M.A. Faghihi Sani, M.R. Mohammadi, Vacuum, 108 (2014) 12-19.

[8] X. Kang, T. Xin, F. Jin, L. Dong, W. Zhao, Aircraft Engineering and Aerospace Technology: An International Journal, 83/1 (2011) 21-25.
[9] A.L. Yerokhin, A. Shatrov, V. Samsonov, P. Shashkov, A. Pilkington, A. Leyland, A. Matthews, Surface and Coatings Technology, 199 (2005) 150-157.
[10] S.A. Karpushenkov, A.I. Kulak, G.L. Shchukin, A.L. Belanovich, Protectionof Metals and Physical Chemistry of Surfaces, 46 (2010) 463–468.
[11] J.B. Bajat, R. Vasilić, S. Stojadinović, V. Mišković-Stankovic, Corrosion, 69 (2013) 693-702.
[12] A. Bahramian, K. Raeissi, A. Hakimizad, Applied Surface Science, 351 (2015) 13-26.
[13] R.H.U. Khan, A.L. Yerokhin, A. Matthews, Philosophical Magazine, 6 (2008) 795–807.
[14] A. Hakimizad, K. Raeissi, M.A. Golozar, X. Lu, C. Blawert, M.L. Zheludkevich, Surface and Coatings Technology, 324 (2017) 208-221.
[15] S.P. Sah, E. Tsuji, Y. Aoki, H. Habazaki, Corrosion Science, 55 (2012) 90-96.
[16] Y.-l. Cheng, Z.-g. Xue, Q. Wang, X.-Q. Wu, E. Matykina, P. Skeldon, G.E. Thompson, Electrochimica Acta, 107 (2013) 358-378.
[17] X. Chen, Q. Cai, L. Yin, in: Advanced Materials Research, 2012, pp. 1969-1975.
[18] H. Duan, C. Yan, F. Wang, Electrochimica Acta, 52 (2007) 3785-3793.
[19] A. Fattah-Alhosseini, M. Vakili-Azghandi, M.K. Keshavarz, Acta Metallurgica Sinica (English Letters), 29 (2016) 274-281.
[20] A. Seyfoori, S. Mirdamadi, Z.S. Seyedraoufi, A. Khavandi, M. Aliofkhazraei, Materials Chemistry and Physics, 142 (2013) 87-94.
[21] D. Sreekanth, N. Rameshbabu, K. Venkateswarlu, C. Subrahmanyam, L. Rama Krishna, K. Prasad Rao, Surface and Coatings Technology, 222 (2013) 31-37.
[22] X. Wu, X. Wang, R. Wang, Harbin Gongye Daxue Xuebao/Journal of Harbin Institute of Technology, 45 (2013) 80-84.
[23] W. Yang, B.-l. Jiang, H.-y. Shi, L.-y. Xian, J. Cent. South Univ. Technol., 17 (2010) 223-227.
[24] Y.M. Kim, D.Y. Hwang, C.W. Lee, B. Yoo, D.H. Shin, Journal of Korean Institute of Metals and Materials, 48 (2010) 49-56.
[25] X. Lu, C. Blawert, Y. Huang, H. Ovri, M.L. Zheludkevich, K.U. Kainer, Electrochimica Acta, 187 (2016) 20-33.
[26] X. Lu, M. Mohedano, C. Blawert, E. Matykina, R. Arrabal, K.U. Kainer, M.L. Zheludkevich, Surface and Coatings Technology, 307, Part C (2016) 1165-1182.
[27] X. Lu, C. Blawert, M.L. Zheludkevich, K.U. Kainer, Corrosion Science, 101 (2015) 201-207.
[28] X. Lu, M. Schieda, C. Blawert, K.U. Kainer, M.L. Zheludkevich, Surface and Coatings Technology, 307, Part A (2016) 287-291.
[29] X. Lu, C. Blawert, M. Mohedano, N. Scharnagl, M.L. Zheludkevich, K.U. Kainer, Surface and Coatings Technology, 289 (2016) 179-185.
[30] N. Xiang, R.G. Song, C. Wang, Q.Z. Mao, Y.J. Ge, J.H. Ding, Corrosion Engineering Science and Technology, 51 (2016) 146-154.
[31] N. Tadić, S. Stojadinović, N. Radić, B. Grbić, R. Vasilić, Surface and Coatings Technology, 305 (2016) 192-199.
[32] V. Dehnavi, D.W. Shoesmith, B.L. Luan, M. Yari, X.Y. Liu, S. Rohani, Materials Chemistry and Physics, 161 (2015) 49-58.
[33] X. Lu, S.P. Sah, N. Scharnagl, M. Störmer, M. Starykevich, M. Mohedano, C. Blawert, M.L. Zheludkevich, K.U. Kainer, Surface and Coatings Technology, 269 (2015) 155-169.
[34] V. Raj, M. Mubarak Ali, Journal of Materials Processing Technology, 209 (2009) 5341-5352.

[35] M. Montazeri, C. Dehghanian, M. Shokouhfar, A. Baradaran, Applied Surface Science, 257 (2011) 7268-7275.
[36] S.V. Gnedenkov, O.A. Khrisanfova, A.G. Zavidnaya, S.L. Sinebryukhov, V.S. Egorkin, M.V. Nistratova, A. Yerokhin, A. Matthews, Surface and Coatings Technology, 204 (2010) 2316-2322.
[37] R.O. Hussein, D.O. Northwood, X. Nie, Journal of Alloys and Compounds, 541 (2012) 41-48.
[38] Y.-j. Guan, Y. Xia, Transactions of Nonferrous Metals Society of China, 16 (2006) 1097-1102.
[39] C.-C. Tseng, J.-L. Lee, T.-H. Kuo, S.-N. Kuo, K.-H. Tseng, Surface and Coatings Technology, 206 (2012) 3437-3443.
[40] S. Stojadinović, R. Vasilić, N. Radić, N. Tadić, P. Stefanov, B. Grbić, Applied Surface Science, 377 (2016) 37-43.
[41] H. Zheng, Y. Wang, B. Li, G. Han, Materials Letters, 59 (2005) 139-142.
[42] R. Mann, W.E.G. Hansal, S. Hansal, Transactions of the Institute of Metal Finishing, 92 (2014) 297-304.
[43] K.M. Lee, K.R. Shin, S. Namgung, B. Yoo, D.H. Shin, Surface and Coatings Technology, 205 (2011) 3779-3784.
[44] A. Timoshenko, B. Opara, Y. Magurova, Zashch. Met., 30 (1994) 32-38.
[45] A. Vladimirovich Timoshenko, Y. Vladimirovna Magurova, Revista de Metalurgia, 36 (2000) 323-330.
[46] A. Venugopal, R. Panda, S. Manwatkar, K. Sreekumar, L.R. Krishna, G. Sundararajan, Transactions of Nonferrous Metals Society of China, 22 (2012) 700-710.
[47] P. Bala Srinivasan, J. Liang, R.G. Balajeee, C. Blawert, M. Störmer, W. Dietzel, Applied Surface Science, 256 (2010) 3928-3935.
[48] L. Wen, Y.M. Wang, Y. Liu, Y. Zhou, L.X. Guo, J.H. Ouyang, D.C. Jia, Corrosion Science, 53 (2011) 618-623.
[49] N. Xiang, R.G. Song, H. Li, C. Wang, Q.Z. Mao, Y. Xiong, Journal of Materials Engineering and Performance, 24 (2015) 5022-5031.
[50] C. Liu, P. Liu, Z. Huang, Q. Yan, R. Guo, D. Li, G. Jiang, D. Shen, Surface and Coatings Technology, 286 (2016) 223-230.

***Suggested Reviewers**

1- Massimiliano Bestetti

Dipartimento di Chimica, Materiali ed Ingegneria Chimica "G. Natta", Politecnico di Milano

Massimiliano.bestetti@polimi.it

Phone:+39-02-23993166 fax: +39-02-23993180

2- Thierry Belmonte

Département Chimie et Physique des Solides et des Surfaces (CP2S)

thierry.belmonte@univ-lorraine.fr

Téléphone: + 33 3 83 58 40 91

3- Aleksey Yerokhin

University of Manchester, School of Materials, Manchester, United Kingdom

A.Yerokhin@sheffield.ac.uk

Aleksey.yerokhin@manchester.ac.uk

4- Peter Skeldon

University of Manchester, Corrosion and Protection Centre, Manchester, United Kingdom

p.skeldon@manchester.ac.uk